Traffic 2006; 7: 205–215
Blackwell Munksgaard



doi: 10.1111/j.1600-0854.2005.00377.x

# Dynamics of Membrane Clathrin-Coated Structures During Cytokinesis

**Anne K. Warner[1], James H. Keen[2] and Yu-Li Wang[1,*]**

*[1]Department of Physiology, University of Massachusetts Medical School, 377 Plantation Street, Worcester, MA 01605, USA*
*[2]Kimmel Cancer Institute, Thomas Jefferson University, Philadelphia, PA 19107, USA*
**Corresponding author: Yu-Li Wang, yuli.wang@umassmed.edu*

**Remodeling of cell membranes takes place during motile processes such as cell migration and cell division. Defects of proteins involved in membrane dynamics, including clathrin and dynamin, disrupt cytokinesis. To understand the function of clathrin-containing structures (CCS) in cytokinesis, we have expressed a green fluorescent protein (GFP) fusion protein of clathrin light chain a (GFP-clathrin) in NRK epithelial cells and recorded images of dividing cells near the ventral surface with a spinning disk confocal microscope. Punctate GFP-CCS underwent dynamic appearance and disappearance throughout the ventral surface. Following anaphase onset, GFP-CCS between separated chromosomes migrated toward the equator and subsequently disappeared in the equatorial region. Movements outside separating chromosomes were mostly random, similar to what was observed in interphase cells. Directional movements toward the furrow were dependent on both actin filaments and microtubules, while the appearance/disappearance of CCS was dependent on actin filaments but not on microtubules. These results suggest that CCS are involved in remodeling the plasma membrane along the equator during cytokinesis. Clathrin-containing structures may also play a role in transporting signaling or structural components into the cleavage furrow.**

**Key words: actin, clathrin, cytokinesis, endocytosis, membrane recycling, microtubules**

**Received 21 June 2005, revised and accepted for publication 1 November 2005, published on-line 12 December 2005**

Cytokinesis, the final step of cell division, is a highly dynamic process involving signaling, cortical contractions, membrane remodeling and vesicle trafficking (1–7). For animal cells, the prevalent model suggests that cytokinesis is achieved primarily by localized contractions, which pinch a cell into two along the equator (6,7). However, the actual mechanism is likely to be more complicated (7). For example, budding of *Sacharromyces cerevisiae* can take place in the absence of myosin II (8), while *Dictyostelium discoideum* amoebae were also able to divide in the absence of myosin II as long as the cell was attached to a solid surface (9). Moreover, cytokinesis of cultured mammalian cells appeared to be facilitated by localized disruption of the actin cytoskeleton along the equator (10), contrary to what one might expect from a simple equatorial contraction model.

For higher plant cells, attention on the mechanism of cytokinesis has long been focused on exocytotic secretion and construction of a new cell wall, guided by the actin filaments and microtubules that concentrate in the equatorial region (11,12). However, similar membrane events may play a global role in cytokinesis, as suggested by the failure of division in *Schizosaccharomyces pombe* upon the inhibition of cell wall synthesis (13). Even in the absence of a cell wall, membrane addition and localized exocytosis near the furrow base have been identified as an important process for the completion of cytokinesis (2,14–16).

In addition to exocytosis, cytokinesis may involve endocytosis and other dynamic membrane events (1,2) as indicated by the cytokinetic failure of cells with mutations in the membrane-trafficking proteins clathrin (17,18), dynamin (19,20) and some Golgi-associated proteins (21). Furthermore, Arf6 and Rab11, small GTPases that regulate endosomal membrane dynamics, have been implicated in cytokinesis based on their localization in the cleavage furrow and effects of RNAi (22,23). Experiments with zebra fish embryos also demonstrated active endocytosis in the furrow region and failure of cytokinesis upon inhibition of endocytosis (24). Proteomic analysis further identified a large number of components for endocytosis in the furrow region (25). However, despite strong evidence, it is not clear how endocytosis fits into the current model that emphasizes cortical pinching and membrane addition rather than removal during ingression.

Much is known about clathrin and its functions in the endocytosis of interphase cells (26–28). Membrane clathrin-containing structures (CCS) show random movements, in addition to budding, appearance, and disappearance (29). Since clathrin plays an essential role in cytokinesis for *Dictyostelium* in suspension (17,18), new insights into the mechanism of cytokinesis may be gained by studying its dynamics during cell division. Curiously, despite its functional role in cytokinesis, there was no clear concentration of clathrin in the cleavage furrow of *Dictyostelium* (30). In the present study, we have used cells expressing GFP-tagged clathrin light chain a to follow the dynamics of CCS during late mitosis

and cytokinesis. We found that a large fraction of CCS in the region between separated chromosomes migrated toward the equator and disappeared in the furrow region. This directional movement of CCS likely drives a crucial membrane remodeling and/or signaling process during cell division.

## Results

### *Distribution of GFP-clathrin on the membrane of dividing NRK cells*

To investigate the dynamics of clathrin-coated structures on the membrane of dividing cells, NRK cells were transfected with plasmids encoding GFP-clathrin light chain a (29). Images were collected near the ventral membrane with spinning disk confocal optics. GFP-clathrin was found as discrete punctate structures over the entire ventral surface during prometaphase, metaphase and early anaphase. During cytokinesis, GFP-clathrin showed a lower concentration along the equator than elsewhere (Figure 1A, lower panel; see also Figure 4). The distribution of GFP-clathrin is similar to that of endogenous clathrin as detected by immunofluorescence staining (data not shown).

To confirm that we were focusing on GFP-clathrin near the plasma membrane, transfected cells were fixed and counter-stained with antibodies against the adaptor protein AP-2, a known component of plasma membrane-associated CCS but not *trans*-Golgi network or cytoplasmic clathrin-coated vesicles (31,32). As shown in Figure 1B, sharply focused GFP-CCS on the ventral surface colocalized extensively with punctate AP-2 structures. However, the amount of AP-2 varied among GFP-CCS, possibly reflecting CCS at different stages of internalization (33,34).

To rule out the possibility that some equatorial CCS might have escaped our detection due to the narrow depth of field of the confocal optics, cells were fixed and optically sectioned from the ventral to the dorsal surface. None of the optical sections showed a concentration of GFP-clathrin along the equator. Reconstructed 90° views, superimposing both CCS and cytoplasmic clathrin-coated

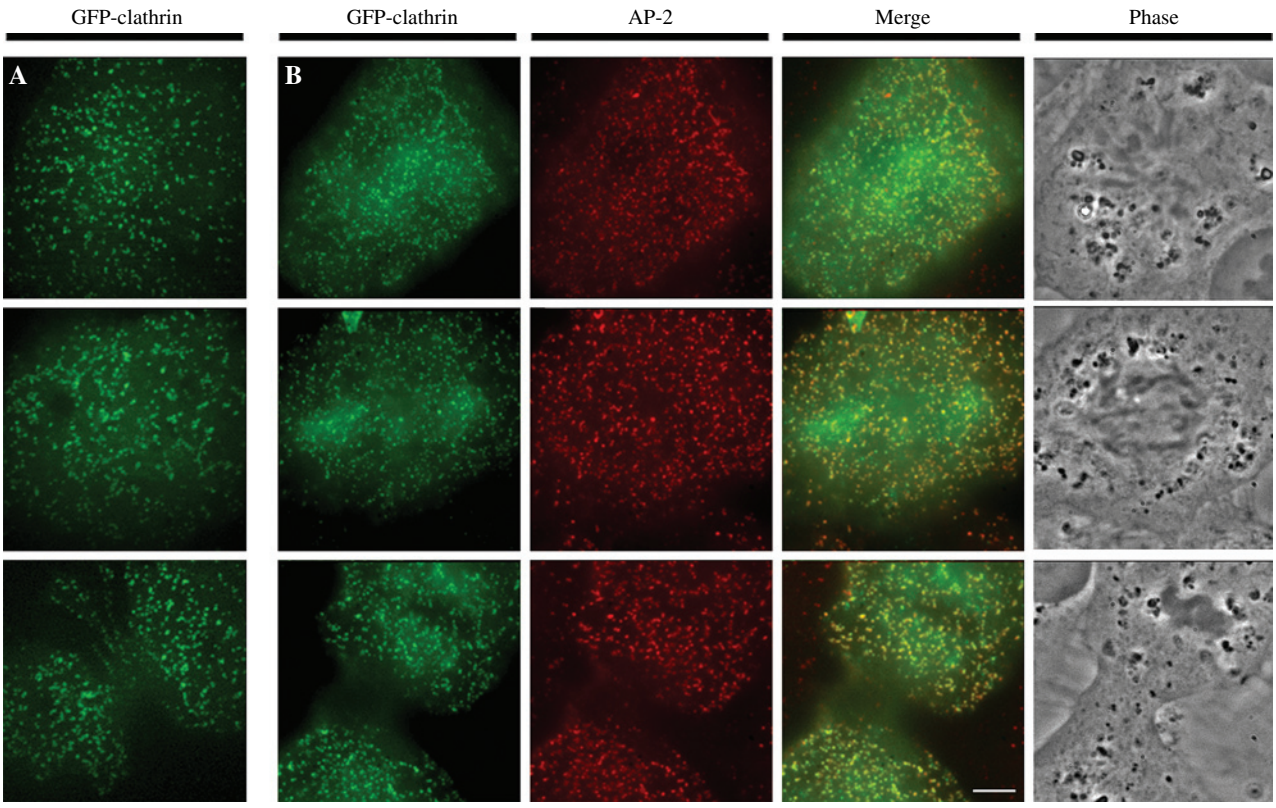


**Figure 1: Imaging clathrin-containing structures near the ventral surface.** The bottom surfaces of NRK cells, transfected with plasmids encoding green fluorescent protein (GFP)-clathrin light chain a, were imaged during prometaphase (top row), early anaphase (middle row) and late anaphase/cytokinesis (bottom row). Images of a living cell acquired by spinning disc confocal microscopy show discrete punctate structures that were less concentrated in the furrow (A). To determine the relationship between the distribution of GFP-clathrin and AP-2, which is known to localize at clathrin-containing structures (CCS), transfected cells were fixed and counter-stained with antibodies against the adaptor protein AP-2 (B). Conventional optics is used for the dual-wavelength comparison between GFP-clathrin and stained AP-2. GFP-clathrin colocalizes extensively with AP-2 on the ventral surface, while out-of-focus GFP-clathrin in the mitotic spindle shows no correlation with the distribution of AP-2. Bar, 5.0 μm.

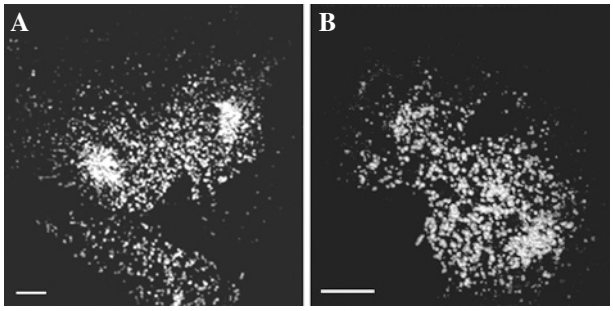


**Figure 2: Lack of accumulation of green fluorescent protein (GFP)-clathrin-containing structures (CCS) in the cleavage furrow.** NRK cells transfected with GFP-clathrin were fixed and optically sectioned. Images of two different cells were reconstructed to show the 90° projection of GFP-clathrin detected on all focal planes. The lack of concentration along the furrow rules out the possibility that some equatorial clathrin structures have escaped detection due to the narrow depth of field. Clathrin-coated vesicles are concentrated at the spindle pole. Bar, 5.0 μm.

vesicles, showed random distribution of structures except for the concentration of vesicles near spindle poles (Figure 2). Similar results were obtained by reconstructing optical sections from fixed cells stained with anti-clathrin or AP-2 antibodies (not shown).

The distribution of GFP-clathrin was further compared with that of dynamin, which is known to interact with CCS and is also required for cytokinesis (20). Figure 3B shows that, as for clathrin, there was no obvious concentration of dynamin in the midzone or furrow region of NRK cells. In addition, dynamin showed a partial colocalization with GFP-clathrin (yellow dots in Figure 3B, right panel). Similar results were obtained with either a monoclonal antibody against dynamin II or MC-53/MC-65 pan dynamin polyclonal antibodies (20). We have also compared the distribution of GFP-clathrin with caveolin, a major component of membrane caveolae (35). Figure 3A revealed that caveolin is localized at punctate structures distinct from the GFP-CCS.

### *Dynamics of GFP-clathrin on the membrane of dividing NRK cells*

The dynamics of GFP-CCS near the ventral membrane was monitored by time-lapse recording with spinning disk confocal optics. Figure 4 shows selected frames of a representative cell from anaphase through early cytokinesis. Upon anaphase onset, GFP-CCS in the region between separating chromosomes (broken lines) started to move toward the equator, while most CCS outside this region defined by separated chromosomes showed no long-range directional movement (Supplemental Videos 1 and 2). This region between separated chromosomes, which widens as anaphase progresses, will be referred to as the active area.

At a given time-point, approximately 65% of GFP-CCS in the active area were found to undergo directional movements. Plots of velocity vectors indicate that all the long range (>0.5 μm) movements were directed toward the equator (Figure 5), although the movement may be

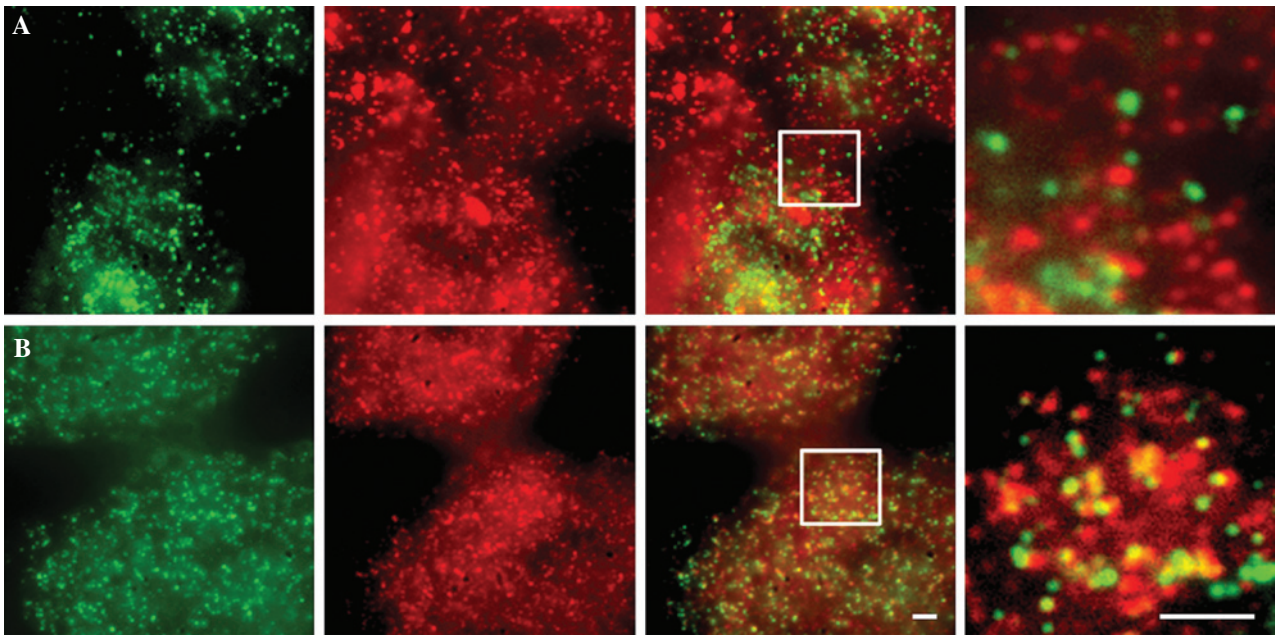


**Figure 3: Partial colocalization of green fluorescent protein (GFP)-clathrin-containing structures (CCS) with dynamin but not with caveolin.** NRK cells were fixed and processed for immunofluorescence with anti-caveolin antibodies (A) or anti-dynamin antibodies (B). GFP-clathrin (green) shows extensive colocalization with dynamin (B, red), but not caveolin (A, red). Far right images show a magnified view of the boxed areas, with colocalization appearing as yellow punctate structures. Bar, 2.0 μm.

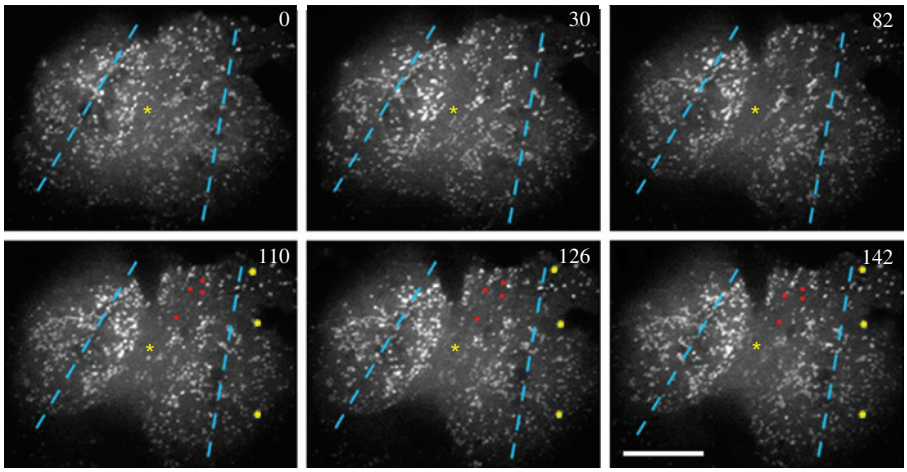


**Figure 4: Movements of green fluorescent protein (GFP)-clathrin-containing structures (CCS) toward the equator.** NRK cells were transfected with plasmids encoding GFP-clathrin light chain a. GFP-CCS near the ventral surface were imaged by spinning disc confocal microscopy from early anaphase through cytokinesis. The cell surface can be divided into two regions indicated by dashed lines: the active area where CCS undergo directional migration toward the equator (red dots in lower panels) and the inactive region where CCS move randomly (yellow dots in lower panels). Asterisk marks a fixed point of reference. The active area matches roughly the region between separated chromosomes (broken lines). Numbers in the upper right corner of each panel show time in seconds after the first panel. Note that despite the movement of GFP-clathrin structures toward the furrow, there is no apparent concentration of clathrin along the equator. See also Supplemental Video 1 available online at http://www.blackwell-synergy.com. Bar, 5.0 μm.

superimposed with short-range (<0.5 μm) random movement (Figure 6A). In addition, while CCS moved predominantly along the long axis of the cell during early cytokinesis (Figure 5), those near the cell border typically migrated parallel to the border thus at an angle from the long axis as ingression progresses (Supplemental Videos 1 and 2). Neighboring CCS often migrated at different rates, and actively moving CCS may be in close proximity to stationary structures (Figure 6A and Supplemental Video 2), suggesting that the movement was driven by a site-specific process rather than by a global cortical flow. Analysis of the trajectories of individual CCS yielded an average rate of approximately 1.92 ± 0.06 μm/min (SEM; $n = 125$ in 14 cells). In contrast, GFP-CCS outside the active area showed primarily random movements with a lower rate (1.26 ± 0.09 μm/min, SEM; $n = 68$ in 11 cells; Figure 6B and Supplemental Video 3), similar to what was found on the surface of interphase cells (29). The difference in speed is statistically significant ($p < 10^{-7}$).

The above observations raised the question why GFP-CCS showed no concentration in the furrow despite their movements toward the equator. Figure 7 and Supplemental Videos 4 and 5 revealed that GFP-CCS underwent dynamic appearance and disappearance, with

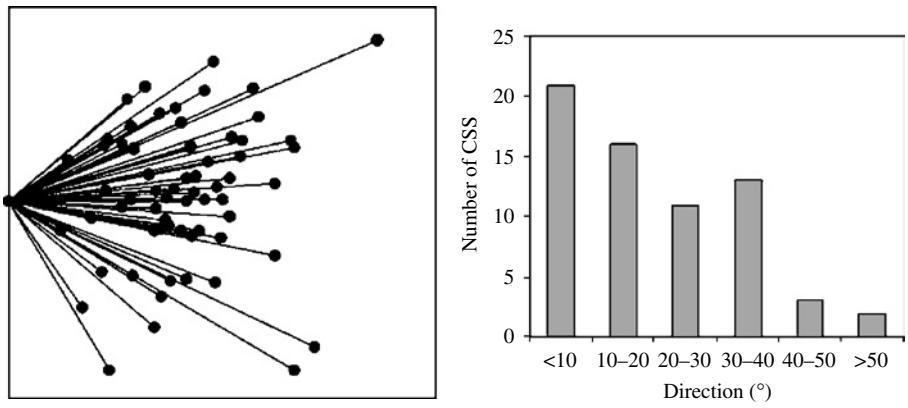


**Figure 5: Distribution of the direction of long-range clathrin-containing structure (CCS) movements in the active region during early cytokinesis.** Left panel shows velocity vectors of 65 randomly selected moving CCS in seven cells. The position and angle of the vectors have been adjusted such that the equator lies along the vertical plane to the right of the CCS and all the movements start from the center of the left edge. Right panel shows histogram of the absolute value of the angle. Most CCS migrate at a shallow angle from the long axis of the cell, which is oriented along 0°.

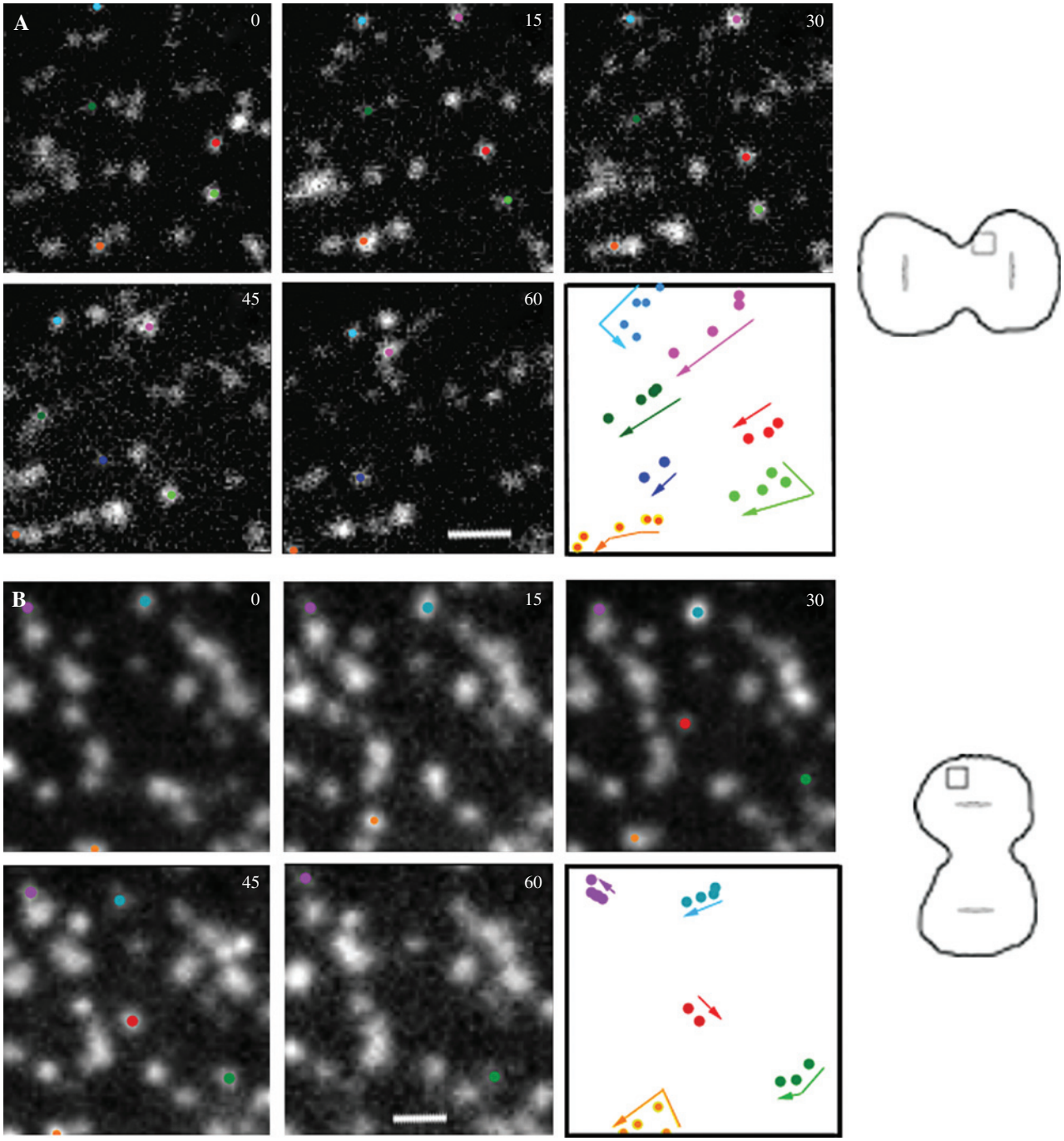


**Figure 6: Migration pattern of green fluorescent protein (GFP)-clathrin-containing structures (CCS) in the active area and inactive area.** Boxes in the schematic diagrams indicate the approximate regions imaged. Colored dots indicate selected GFP-clathrin structures, whose trajectories of movement are shown in the last panel. Arrows in the last panel indicate the direction of movement of each dot. While all the labeled dots in the active area moved toward the furrow (A), the rate and pattern of movement vary between neighboring dots. The region also contained non-moving dots adjacent to moving dots. In the inactive area of a different cell (B), dots moved in random directions. Time in seconds after the first panel is indicated in the upper right corner of each panel. See Supplemental Videos 2 and 3, available online at http://www.blackwell-synergy.com. Bar, 1.0 μm.

a significantly higher rate for disappearance than for appearance in the active area (Figures 7C; $p < 0.00005$). Thus, the increase in equatorial CCS due to directional movement was more than offset by the higher frequency of disappearance in the active region. The frequency of appearance and disappearance was similar outside the active area (Figure 7C; $p = 0.4$). Appearance of most CCS occurred at fixed sites, through what appeared to

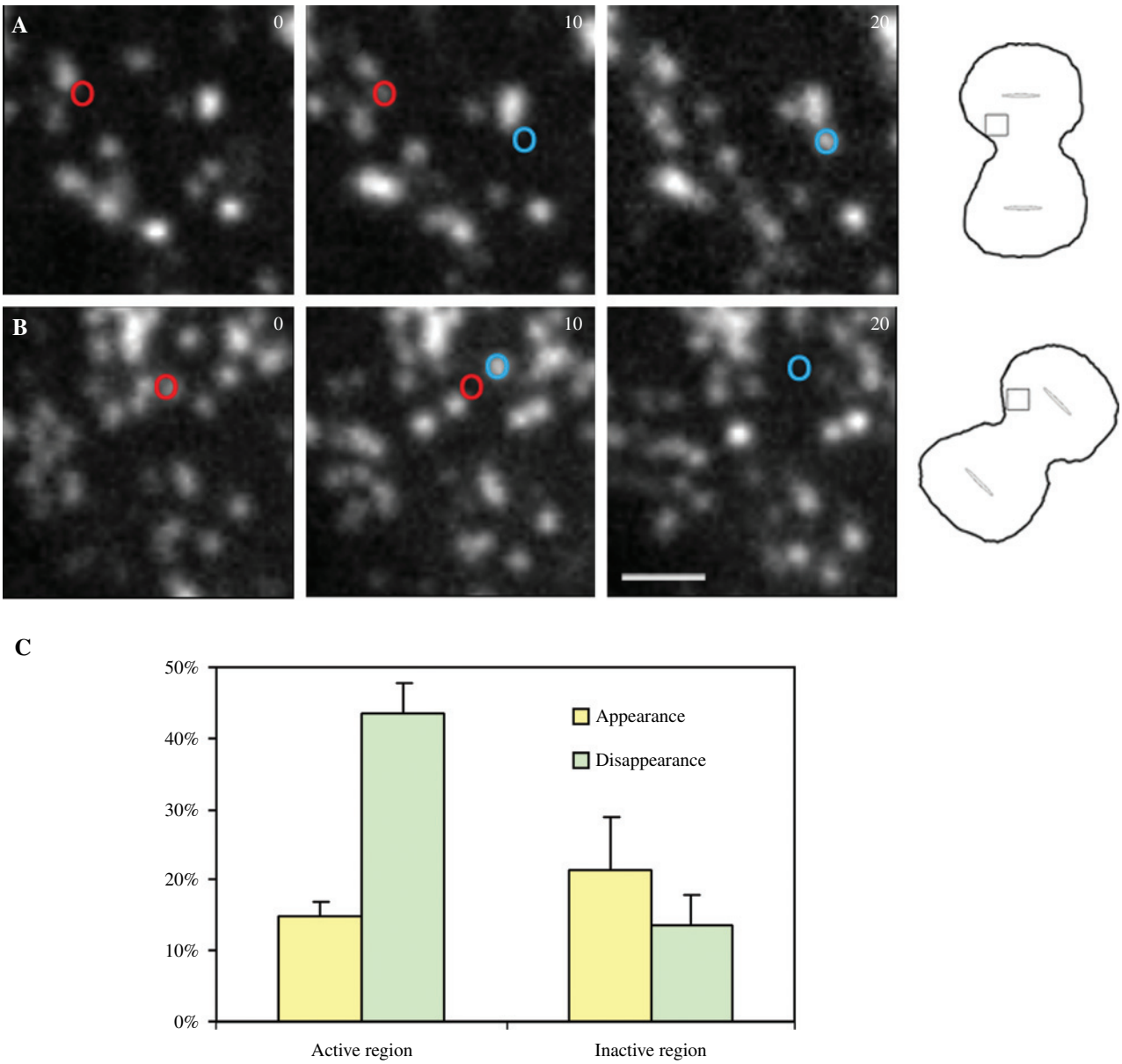


**Figure 7: Dynamic appearance (A) and disappearance (B) of green fluorescent protein (GFP)-clathrin-containing structures (CCS) during cell division.** Boxes in the schematic diagrams indicate the approximate regions imaged. Colored circles indicate individual structures. New CCS appear primarily through budding off existing structures at fixed sites (A). Time in seconds after the first panel is indicated in the upper right corner of each panel. See Supplemental Videos 4 and 5 available online at http://www.blackwell-synergy.com. Bar, 1.0 μm. Analysis of the percentage of appearance and disappearance within a 60–75-second period indicates a higher rate of CCS disappearance in the active area than in the inactive area (C). Bars indicate mean ± SEM.

be a budding process off existing structures (Figure 7A and Supplemental Video 4).

To determine if the high rate of disappearance of CCS in the active area reflects increased endocytosis, cells were pulse-treated with fluorescently labeled transferrin or dextran upon the onset of anaphase and fixed immediately. There was no detectable concentration of transferrin or dextran-containing vesicles in the active area (Figure 8), suggesting that either the disappearance is unrelated to endocytosis or endocytic vesicles were transported out of the furrow region at a high rate.

### *Dependence of the directional movement of CCS on cytoskeletal structures*

To test if the directional movement of GFP-CCS was dependent on microtubules, cells were treated with nodocazole upon anaphase onset (Figure 9A). The treatment inhibited directional movements in the active region, although appearance/disappearance activities of CCS

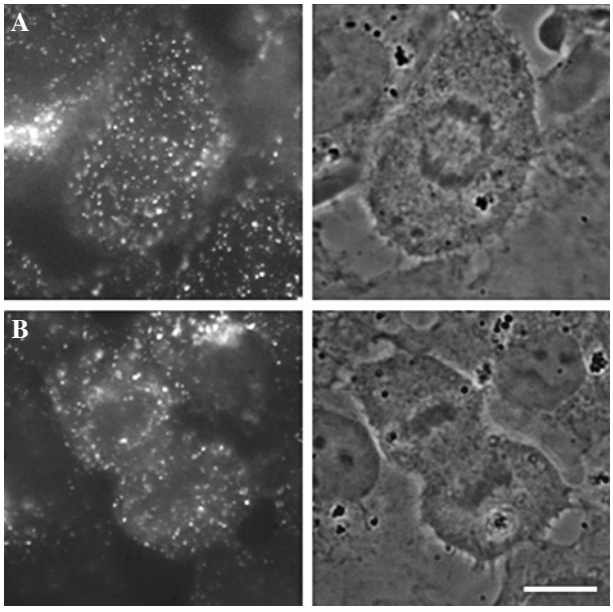


**Figure 8: Distribution of endocytic vesicles in dividing cells.** NRK cells were fixed after incubating 3–5 min with Texas-red-labeled transferrin and imaged by conventional fluorescence microscopy. The transferrin signal is relatively uniform during anaphase (A) and cytokinesis (B) in two separate cells. Bar, 10.0 μm.

persisted (arrows, Figure 9A and Supplemental Video 6). A more complete inhibition of both CCS movement and appearance/disappearance activities was observed when the actin cytoskeleton was disrupted with either 5 μM latrunculin A or 5 μM cytochalasin D (Figure 9B and Supplemental Video 7). These observations indicate that the directional movement of GFP-CCS requires both intact actin filaments and microtubules.

## Discussion

### *Dynamics of membrane CCS during cytokinesis*

Previous studies have characterized the movement of CCS during interphase (29,36,37). The present results indicate that such movements persisted during mitosis until anaphase onset. However, the most striking finding is that a large fraction of CCS in the region between separated chromosomes undergoes directional migration toward the equator during anaphase and telophase. Neighbouring CCS moved asynchronously and independently, suggesting that a site-specific process drove the movement and/or anchored some CCS. In addition, the colocalization of clathrin and AP-2 (Figure 1) and the similar behavior of AP-2 as observed with a GFP construct (unpublished observations) suggest that the dynamics of clathrin involved the turnover and migration of the entire CCS.

Despite the directional migration into the furrow region, there was no apparent accumulation of CCS along the equator. A similar lack of concentration of clathrin in the cleavage furrow was shown previously in *Dictyostelium* (30), while clathrin appeared to be concentrated in the cleavage furrow of zebra fish embryos (24). In addition, dynamin, a protein closely associated with clathrin during membrane budding, was found to concentrate in the furrows of *Caenorhabditis elegans* embryos and a rat liver cell line (20). Our results suggest that the pattern of CCS distribution is determined by the combination of directional migration and disappearance of CCS along the equator (Figures 4–7). Equatorial concentration of CCS proteins takes place when the influx due to directed transport exceeds the rate of disappearance. The differences among embryos and various cell lines may thus reflect different rates of CCS migration relative to disassembly.

As for CCS movements in interphase cells (36,37), directional transport of CCS was dependent upon an intact actin and microtubule cytoskeleton. Furthermore, the active region corresponded to the spindle interzone, which formed upon anaphase onset and contained a set of organized microtubules referred to as interzonal microtubules (3). We found that some CCS are aligned along interzonal microtubules (not shown), while a recent study showed the association of clathrin heavy and light chains, but not the adaptor proteins, with kinetochore microtubules during mitosis (38). The sensitivity of CCS movement to the microtubule-destabilizing agent nocodazole further suggested that the movement may be guided at least partially by these interzonal microtubules. The dependence of directed movements of CCS on both actin filaments and microtubules may reflect the physical link between actin and microtubule networks as has been demonstrated on the cortex of oocytes (39).

### *Functions of membrane CCS during cytokinesis*

In interphase cells, the disappearance of CCS reflected the pinching and uncoating of endocytic vesicles (29). Thus, one may interpret the disappearance of CCS in the cleavage furrow as an indication of elevated endocytic activities, which was shown along the equator of zebra fish embryos (24). The involvement of endocytosis in cytokinesis is also supported by the defects in cytokinesis following the disruption of a number of proteins required for endocytosis, including dynamin, Arf6 and Rab11 (19–23).

While the involvement of exocytosis in cytokinesis has long been recognized as a means for providing the membrane for increased surface area during cell division (2,14,15), it is not readily apparent how equatorial endocytosis fits into the current model of cytokinesis. One possibility is that both endocytosis and exocytosis are required for remodeling the plasma membrane, e.g. to cause changes in the composition of the membrane lipids and/or associated proteins. Clathrin-containing structures contain cholesterol and possibly other special lipids, and clathrin-dependent membrane remodeling in the furrow region may mediate the enrichment of sterols required

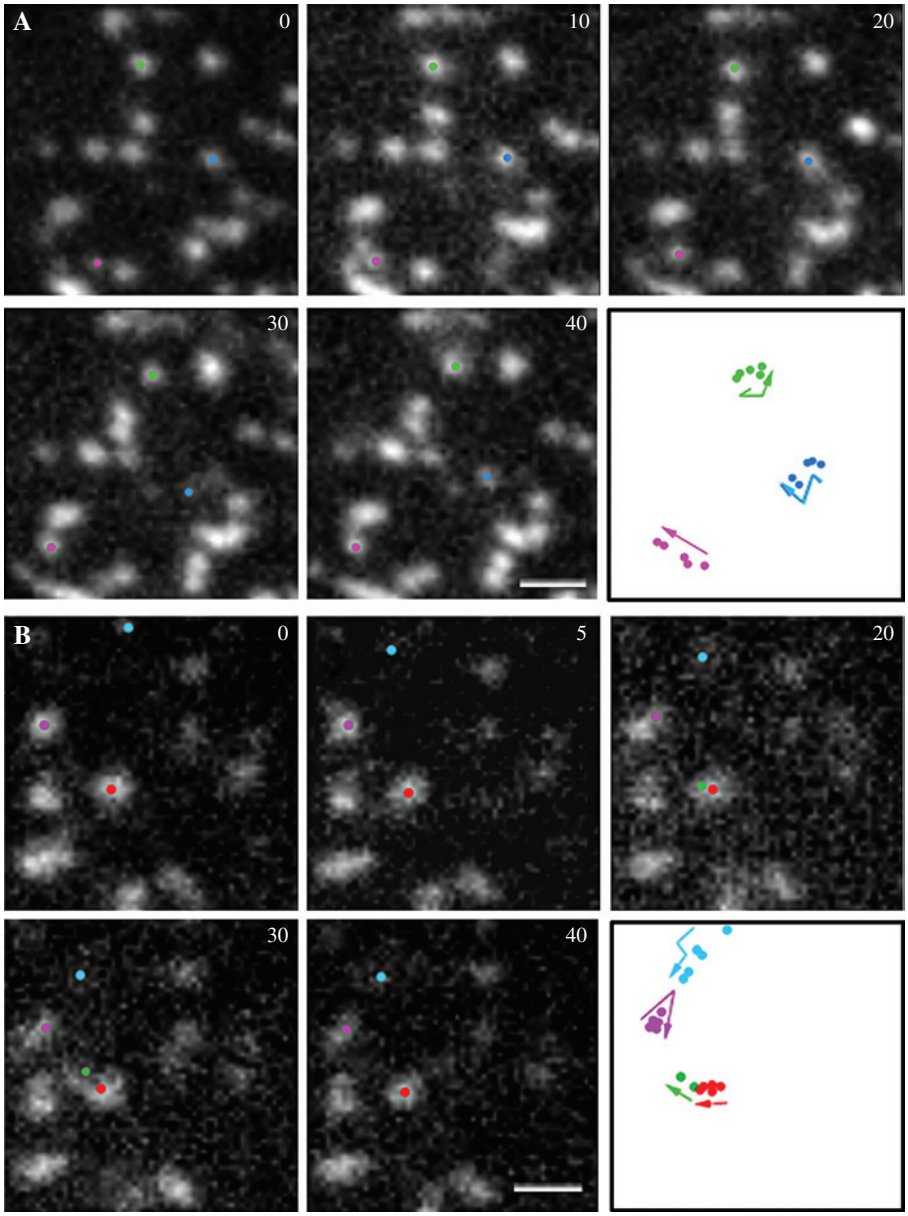


**Figure 9: Requirement of intact microtubules and actin filaments for the directional movement of green fluorescent protein (GFP)-clathrin-containing structures (CCS).** NRK cells transfected with plasmids encoding GFP-clathrin light chain a were treated with either 3.3 μM nocodazole (A) or 5 μM cytochalasin D (B) after anaphase onset. Images were collected near the ventral surface in an area that would exhibit directional movement in control cells. Both treatments cause inhibition of directional movement of GFP-CCS toward the equator; however, random movements persist. Time in seconds after the first panel is indicated in the upper right corner of each panel. See Supplemental Videos 6 and 7 available online at http://www.blackwell-synergy.com. Bar, 1.0 μm.

for cytokinesis (40,41). In addition, membrane remodeling may be responsible for the exposure of phosphatidylethanolamine (42), which is normally present in the inner leaflet of the plasma membrane, in the cleavage furrow. Depletion of phosphatidylethanolamine from the plasma membrane blocked the completion of cytokinesis, presumably by affecting the disassembly of the actin-contractile ring (42).

A second possibility is that CCS and endocytosis may be involved in the assembly of the equatorial actin cortex. While we and other investigators showed that an intact actin cytoskeleton is required for CCS dynamics (Figure 9) (37), given the close association with the actin cytoskeleton (43,44), CCS may play an important role in the reorganization of the actin cortex and assembly of the contractile ring along the equator. For example, CCS may mediate the recruitment of actin filaments and associated proteins such as cortactin (34). It is noteworthy that the rate and pattern of CCS movement appeared similar to what was found for actin filaments and membrane receptors during cytokinesis (45,46). In addition, the CCS protein dynamin is known to enrich in areas of high membrane dynamic activities and to play a role in cell-shape modulation (44).

A third possibility is that CCS may be involved in the signaling events during cytokinesis. The directional migration of CCS may deliver signaling components to the equatorial region, where they stimulate cortical ingression.

CCS interact with phosphoinositides that regulate cytoskeletal proteins such as profilin and gelsolin (47). The involvement of phosphoinositides in cytokinesis is further suggested by the localization of IP3 kinase in the polar region and PTEN (phosphatase-dephosphorylating phosphoinositides) along the equator and the requirement of these enzymes for cytokinesis (48). Furthermore, phosphatidylinositol 4,5-bisphosphate is concentrated in the cleavage furrow of dividing mammalian cells (49) and may be required for regulating calcium concentration and/or membrane–cortex interactions during cytokinesis (49,50). CCS are also known to regulate other signaling pathways including receptor tyrosine kinases, which may also play a role in regulating cytokinesis (47).

## Materials and Methods

### *Cell culture, transfection and treatments*

A subclone of Normal Rat Kidney cells (NRK-52E; American Type Culture Collection, Rockville, MD, USA) was grown on glass coverslips in Kaighan's modified F12 medium (Sigma, St Louis, MO) supplemented with 10% fetal calf serum (JRH Biosciences, Lenexa, KS, USA), 1 mM L-glutamine, 50 μg/mL streptomycin and 50 U/mL penicillin (Gibco, Grand Island, NY, USA). Cells were maintained at 37 °C in a humidified atmosphere containing 5% $CO_2$. Plasmids for GFP-tagged clathrin light chain a pEGFP-LCa, were described previously (29). Transient transfections were carried out using LipofectAMINE (Gibco), according to the protocol provided by the manufacturer. Cells were imaged 24–48 h after transfection.

For drug treatments, transfected cells at prometaphase or metaphase were followed by phase microscopy until anaphase onset. The medium was then replaced with medium containing drugs (3.3 μM nocodazole, 5 μM latrunculin A or 5 μM cytochalasin D; all from Sigma), after rinsing the cells twice with drug-containing media. To visualize endocytosis, cells were pulse-labeled with Texas-red transferrin (20 μg/mL; Molecular Probes, Eugene, OR, USA) or fluorescein dextran (5 mg/mL; Molecular Probes) at 37 °C for 3–5 min, and then fixed immediately as described below for immunofluorescence.

### *Immunofluorescence staining*

Cells grown on glass coverslips were rinsed twice in warm PBS (137 mM NaCl, 2.7 mM KCl, 8 mM $Na_2HPO_4$ and 1.5 mM $KH_2PO_4$) and then fixed for 10 min with 4% formaldehyde (Electron Microscopy Sciences, Fort Washington, PA, USA) in warm PBS containing 0.1% Triton X-100 (Sigma). For the immunofluorescence of tubulin, 5 μM paclitaxel (Sigma) was included in the fixation solution. Fixed cells were then blocked for at least 45 min by incubation with PBS containing 1% bovine serum albumin (Roche Diagnostics, Indianapolis, IN, USA) and labeled for at least 1 h with primary antibodies in PBS/BSA in a humidified environment. The dilution factors were 1:100 for antibodies against dynamin II (BD Transduction Laboratories, San Jose, CA, USA), 1:200 for MC-63/MC-65 pan dynamin antibodies (kindly provided by Dr M.A. McNiven, Mayo Clinic, Rochester, MN, USA) (51), 1:5 for X-22 anticlathrin heavy chain (29), 1:2 for anti-AP2α subunit (AP.6) (29), 1:200 for anticaveolin (BD Transduction Laboratories) and 1:200 for antitubulin (Sigma). After washing for 45 min with several changes of PBS/BSA, the cells were incubated for 30 min with appropriate secondary antibodies labeled with Alexa-488 or 546 (1:200 in PBS/BSA; Molecular Probes). The cells were rinsed with PBS and placed in an antibleaching cocktail of 0.1% *p*-phenylenediamine (Sigma), 50% glycerol in PBS.

### *Microscopy*

For live-cell imaging, cells were maintained in a custom-stage incubator built on top of an Axiovert S100TV inverted microscope (Carl Zeiss, Thornwood, NY, USA). The microscope was equipped with Plan-Neofluar ×100/1.3 N.A. and ×40/1.3 N.A. oil objectives. Confocal imaging was performed with a Yokogawa spinning disk confocal scan head (model CSU10; Solamere Technology Group, Salt Lake City, UT, USA) illuminated with an argon ion laser (Reliant 150M, Laser Physics, West Jordan, UT) set at 488 nm. Images from live cells were collected at a frequency of 5–10 seconds. All dual-wavelength imaging was performed with conventional optics, using a 100 W mercury arc lamp and filter sets for GFP (Chroma Technology, Brattleboro, VT, USA) or TRITC (Omega Optical, Brattleboro, VT, USA). Optical sectioning was performed using a custom-designed stepper motor under computer control. All images were acquired using a cooled CCD camera (CCD-512-EBFT; Roper Scientific, Trenton, NJ, USA). Background subtraction, three-dimensional reconstruction and generation of merged color images were performed using custom software. Final images were processed with Adobe Photoshop.

### *Image analysis*

To characterize the movement of CCS, GFP-clathrin-containing dots were identified in 4–12 consecutive frames by visual examination of the movie sequence. Trajectories and rates of movement were then calculated based on the coordinates of the center of the dots and the known magnification. Average speed was calculated from at least 40 dots. To calculate the percentage appearance/disappearance of CCS, a square of approximately 2 × 2 μm was placed randomly over selected regions. The number of dots that appeared (including those formed de novo or budded off an existing site) or disappeared over a period of 60–75 seconds was counted within the square and divided by the maximum number of dots found in the square during the same period to obtain the percentage.

## Supplementary Material

The following videos are available as part of the online article from http://www.blackwell-synergy.com

**Video 1:** Overview of CCS dynamics on the ventral surface of a dividing cell as for Figure 4, but from a different cell. Line marks the equator. Duration, 5 min.

**Video 2:** Directional movements of CCS in the active region. See legend of Figure 6A for details. Duration, 3 min 14 seconds.

**Video 3:** Random movements of CCS outside the active region. See legend of Figure 6B for details. Duration, 4 min 50 seconds.

**Video 4:** Dynamic appearance of CCS in the active region. See legend of Figure 7A for details. Duration, 4 min 50 seconds.

**Video 5:** Dynamic disappearance of CCS in the active region. See legend of Figure 7B for details. Duration, 2 min 5 seconds.

**Video 6:** Effects of 3.3 μM nocodazole on the dynamics of CCS. See legend of Figure 9A for details. The treatment causes inhibition of directional movements; however, some appearance/disappearance activities persist. Duration, 6 min 30 seconds.

**Video 7:** Effects of 5 μM cytochalasin D on the dynamics of CCS. See legend of Figure 9B for details. The treatment causes strong inhibition of both directional movements and appearance/disappearance of CCS. Duration, 8 min 15 seconds.

## Acknowledgments

The authors would like to thank Dr Mark McNiven, Mayo Clinic, for providing pan-dynamin antibodies. This study was supported by NIH grants GM-32476 to Y.-L.W and GM-28526 to J.H.K.

## References

1. O'Halloran TJ. Membrane traffic and cytokinesis. Traffic 2000;1:921–926.
2. Albertson R, Riggs B, Sullivan W. Membrane traffic: a driving force in cytokinesis. Trends Cell Biol 2005;15:92–101.
3. Burgess DR, Chang F. Site selection for the cleavage furrow at cytokinesis. Trends Cell Biol 2005;15:156–162.
4. Glotzer M. The molecular requirements for cytokinesis. Science 2005;307:1735–1739.
5. D'Avino PP, Savion MS, Glover DM. Cleavage furrow formation and ingression during animal cytokinesis: a microtubule legacy. J Cell Sci 2005;118:1549–1558.
6. Reichl EM, Effler JC, Robinson DN. The stress and strain of cytokinesis. Trends Cell Biol 2005;15:201–206.
7. Wang YL. The mechanism of cytokinesis: reconsideration and reconciliation. Cell Struct Funct 2001;26:633–638.
8. Bi E, Maddox P, Lew DJ, Salmon ED, McMillan JN, Yeh E, Pringle JR. Involvement of an actomyosin contractile ring in *Saccharomyces cerevisiae* cytokinesis. J Cell Biol 1998;142:1301–1312.
9. Gerisch G, Weber G. Cytokinesis without myosin II. Curr Opin Cell Biol 2000;12:126–132.
10. O'Connell CB, Warner AK, Wang YL. Distinct roles of the equatorial and polar cortices in the cleavage of adherent cells. Curr Biol 2001;11:702–707.
11. Smith LG. Plant cytokinesis: motoring to the finish. Curr Biol 2002;12:R206–R208.
12. Juergens G. Plant cytokinesis: fission by fusion. Trends Cell Biol 2005;15:277–283.
13. Liu J, Wang H, McCollum D, Balasubramanian MK. Drc1p/Cps1p, a 1, 3-beta-glucan synthase subunit, is essential for division septum assembly in *Schizosaccharomyces pombe*. Genetics 1999;153:1193–1203.
14. Danilchik MV, Bedrick SD, Brown EE, Ray K. Furrow microtubules and localized exocytosis in cleaving *Xenopus laevis* embryos. J Cell Sci 2002;116:273–283.
15. Shuster CB, Burgess DR. Targeted new membrane addition in the cleavage furrow is a late, separate event in cytokinesis. Proc Natl Acad Sci USA 2002;99:3633–3638.
16. Skop AR, Bergmann D, Mohler WA, White JG. Completion of cytokinesis in *C. elegans* requires a brefeldin A-sensitive membrane accumulation at the cleavage furrow apex. Curr Biol 2001;11:735–746.
17. Niswonger ML, O'Halloran TJ. A novel role for clathrin in cytokinesis. Proc Natl Acad Sci USA 1997;94:8575–8578.
18. Gerald NJ, Damer CK, O'Halloran TJ, De Lozanne A. Cytokinesis failure in clathrin-minus cells is caused by cleavage furrow instability. Cell Motil Cytoskel 2001;48:213–223.
19. Wienke DC, Knetsch ML, Neuhaus EM, Reedy MC, Manstein DJ. Disruption of a dynamin homologue affects endocytosis, organelle morphology, and cytokinesis in *Dictyostelium discoideum*. Mol Biol Cell 1999;10:225–243.
20. Thompson HM, Skop AR, Euteneuer U, Meyer BJ, McNiven MA. The large GTPase dynamin associates with the spindle midzone and is required for cytokinesis. Curr Biol 2002;12:2111–2117.
21. Sisson JC, Field C, Ventura R, Royou A, Sullivan W. Lava lamp, a novel peripheral golgi protein, is required for *Drosophila melanogaster* cellularization. J Cell Biol 2000;151:905–918.
22. Schweitzer JK, D'Souza-Schorey C. Localization and activation of the ARF6 GTPase during cleavage furrow ingression and cytokinesis. J Biol Chem 2002;277:27210–27216.
23. Wilson GM, Fielding AB, Simon GC, Yu X, Andrew PD, Hames RS, Frey AM, Peden AA, Gould GW, Prekeris R. The FIG3-Rab11 protein complex regulates recycling endosome targeting to the cleavage furrow during late cytokinesis. Mol Biol Cell 2005;16:849–860.
24. Feng B, Schwartz H, Jesuthasan S. Furrow-specific endocytosis during cytokinesis of zebrafish blastomeres. Exp Cell Res 2002;279: 14–20.
25. Skop A, Liu H, Yates J, Meyer BJ, Heald R. Dissection of the mammalian midbody proteome reveals conserved cytokinesis mechanism. Science 2004;305:61–66.
26. Schmid S. Clathrin-coated vesicle formation and protein sorting: an integrated process. Annu Rev Biochem 1997;66:511–548.
27. Kirchhausen T. Clathrin. Annu Rev Biochem 2000;69:699–727.
28. Mousavi SA, Malerod L, Berg T, Kjeken R. Clathrin-dependent endocytosis. Biochem J 2004;377:1–16.
29. Gaidarov I, Santini F, Warren RA, Keen JH. Spatial control of coated-pit dynamics in living cells. Nature Cell Biol 1999;1:1–7.
30. Damer CK, O'Halloran TJ. Spatially regulated recruitment of clathrin to the plasma membrane during capping and cell translocation. Mol Biol Cell 2000;11:2151–2159.
31. Takei K, Haucke V. Clathrin-mediated endocytosis: membrane factors pull the trigger. Trends Cell Biol 2001;11:385–391.
32. Smythe E. Regulating the clathrin-coated vesicle cycle by AP2 subunit phosphorylation. Trends Cell Biol 2002;12:352–354.
33. Rappoport JZ, Benmerah A, Simon SM. Analysis of the AP-2 adaptor complex and cargo during clathrin-mediated endocytosis. Traffic 2005;6:539–547.
34. Merrifield CJ, Perrais D, Zenisek D. Coupling between clathrin-coated pits invagination, cortactin recruitment, and membrane scission observed in live cells. Cell 2005;121:593–606.
35. Liu P, Rudick M, Anderson RGW. Multiple functions of caveolin-1. J Biol Chem 2002;277:41295–41298.
36. Rappoport JZ, Taha BW, Simon SM. Movements of plasma-membrane-associated clathrin spots along the microtubule cytoskeleton. Traffic 2003;4:460–467.
37. Yarar D, Waterman-Storer CM, Schmid SL. A dynamic actin cytoskeleton functions at multiple stages of clathrin-mediated endocytosis. Mol Biol Cell 2005;16:964–975.
38. Royle SJ, Bright NA, Lagnodo L. Clathrin is required for the function of the mitotic spindle. Nature 2005;434:1152–1157.
39. Mandato CA, Bement WM. Actomyosin transports microtubules and microtubules control actomyosin recruitment during Xenopus oocyte wound healing. Curr Biol 2003;13:1096–1105.
40. Watchler V, Rajagopalan S, Balasubramanian MK. Sterol-rich plasma membrane domains in the fission yeast *Schizosaccharomyces pombe*. J Cell Sci 2003;116:867–874.
41. Takeda T, Kawate T, Chang F. Organization of a sterol-rich membrane domain by cdc15p during cytokinesis in fission yeast. Nature Cell Biol 2004;6:1142–1144.
42. Emoto K, Umeda M. An essential role for a membrane lipid in cytokinesis: Regulation of contractile ring disassembly by redistribution of phosphatidylethanolamine. J Cell Biol 2000;149:1215–1224.
43. Qualmann B, Kessels MM. Endocytosis and the cytoskeleton. Int Rev Cytol 2002;220:93–144.
44. Schafer DA. Coupling actin dynamics and membrane dynamics during endocytosis. Curr Opin Cell Biol 2002;14:76–81.
45. Cao L, Wang YL. Mechanism of the formation of contractile ring in dividing cultured animal cells. II. Cortical movement of microinjected actin filaments. J Cell Biol 1990;111:1905–1911.
46. Wang YL, Silverman JD, Cao L. Single particle tracking of surface receptor movement during cell division. J Cell Biol 1994;127: 963–971.
47. LeRoy C, Wrana JL. Clathrin- and non-clathrin-mediated endocytic regulation of cell signaling. Nat Rev Mol Cell Biol 2005;6:112–126.

48. Janetopoulos C, Borleis J, Vazquez F, Iijima M, Devreotes P. Temporal and spatial regulation of phosphoinositide signaling mediates cytokinesis. Dev Cell 2005;8:467–477.
49. Field SJ, Madson N, Kerr ML, Galbraith KAA, Kennedy CD, Tahiliani M, Wilkins A, Cantley LC. PtdIns(4,5)P2 functions at the cleavage furrow during cytokinesis. Curr Biol;15:1407–1412.
50. Wong R, Hadjiyanni I, Wei HC, Polevoy G, McBride R, Sem KP, Brill JA. PIP2 hydrolysis and calcium release are required for cytokinesis in *Drosophila* spermatocytes. Curr Biol 2005;15:1401–1406.
51. Henley JR, McNiven MA. Association of a dynamic-like protein with the Golgi apparatus in mammalian cells. J Cell Biol 1996;133: 761–775.